GEOPHYSICAL RESEARCH LETTERS, VOL. 22, NO. 20, PAGES 2837-2840, OCTOBER 15, 1995

Determination of horizontal and vertical structure of an unusual pattern of short period gravity waves imaged during ALOHA-93

M.J. Taylor

Space Dynamics Laboratory and Physics Department, Utah State University

D.C. Fritts and J.R. Isler

Laboratory for Atmospheric and Space Physics, University of Colorado

Abstract. An all-sky CCD imager has been used to measure the properties of short period gravity waves present over the Hawaiian Islands during the ALOHA-93 campaign. Observations of emissions from four different altitudes provided a capability to describe the vertical as well as the horizontal structure of the wave field. On several occasions during this campaign an unusual morphology wave pattern was detected that consisted of a group of small-scale waves oriented in the same direction. These were most noticeable in the OI (557.7 nm) emission, altitude ~96 km, and were usually observed in association with a larger scale gravity wave. This paper presents a preliminary analysis of data recorded on the night of 22 October during which both types of waves were prominent. The small-scale waves exhibited highly coherent phase structures at each emission altitude, consistent with a ducted wave motion. The spatial intensity and phase modulation of this display is indicative of interference between two waves with similar characteristics and slightly different propagation directions. The larger scale wave motion was observed to propagate perpendicular to the small-scale waves, and showed evidence of phase progression with altitude, implying upward energy propagation. These data have been interpreted in the context of simultaneous wind measurements from an MF radar.

Introduction

Since gravity waves were first recognized as an important atmospheric phenomenon [Hines, 1960] considerable observational and theoretical research has ensued. These efforts have established the importance of such motions in driving the mean circulation and thermal structure of the mesosphere and lower thermosphere via wave energy and momentum transports [Fritts, 1989], yet the processes responsible for the variability, interactions and saturation of the gravity wave spectrum remain poorly understood at present. Images of the nightglow emissions from several different layers offer a unique three-dimensional measurement capability for quantifying the effects of small-scale wave motions on the upper mesosphere and lower thermosphere (~80-100 km). Most nightglow image measurements reported in the literature concern short-period motions (<1 hour) and fall into two distinct categories termed "bands" and "ripples". Bands are extensive, long-lasting wave patterns exhibiting horizontal wavelengths (λ_h) of several tens of kilometers and horizontal phase velocities (v_h) of up to 100 ms^{-1} [Clairemidi et al., 1985]. These patterns have been attributed to vertically propagating short-period gravity waves [Taylor et al., 1987]. Ripples are short-lived (<45 min) small-scale wave patterns (λ_h ~5-15 km), of restricted spatial extent [Peterson, 1979], and are thought to be generated in-situ by localized shear instabilities in the wind field [Taylor and Hapgood, 1990]. This paper describes an unusual morphology short-period wave pattern which appears to fall in between these two categories and was observed concurrently with a well-developed band display progressing on an almost orthogonal heading. Both wave motions occupied much of the visible sky at nightglow emission altitudes, but exhibited very different propagation characteristics.

Paper number 95GL02945
0094-8534/95/95GL-02945$03.00

Nightglow and Radar Observations

During the ALOHA-93 campaign (6-23 October, 1993) a high-performance all-sky CCD imaging system was operated at Haleakala Crater (20.8°N, 156.2°W, 2970m) to measure gravity waves within a ~450 km radius of Maui, Hawaii. Sequential observations of the NIR OH(715-930 nm) and O_2(0,1) At bands (centered at ~865 nm) and the OI(557.7 nm) and Na(589.2 nm) line emissions were recorded in a cycle time of ~9 min. Well-defined gravity wave bands and ripple events were observed on many occasions in each of these emissions [Taylor et al., 1995].

On several nights a most unusual wave pattern was imaged consisting of organized groups of small-scale waves, all oriented in the same direction and often extending over a large area of sky. In many cases these waves appeared in association with a set of larger scale bands oriented approximately orthogonal to the smaller-scale structures. This phenomenon was most pronounced on the night of 22 October. Correlative radar wind profiles were also obtained with the Hawaii MF radar located on Kauai, Hawaii (22°N, 160°W), ~375 km to the WNW of Maui. During ALOHA-93 the radar registered considerable amplitude variability of the diurnal tide [Isler and Fritts, 1995]. Here, the radar data have been used to define the average horizontal winds at nightglow altitudes. The winds were averaged over 3 hour intervals in order to focus on motions coherent over the horizontal distance separating the two sites.

22 October Nightglow Wave Display

All four nightglow emissions registered wave structure throughout this night, from 08:30 to 15:30 UT. Figure 1 shows four images of the OI(557.7 nm) nightglow emission illustrating the morphology of these waves at ~96 km altitude. They reveal a dramatic series of wave motions, with the dominant structures at early times consisting of several groups (rows) of small scale, ripple-like, waves but with a large λ_h of 19 ± 0.5 km and lifetimes > 2 hours. Figure 2 plots the position and extent of this wave pattern at 09:27 UT in Figure 1a. Image sequences reveal a phase speed of ~40 ms^{-1} towards the SE (azimuth ~137°) and an apparent drift of the wave group towards the NE (azimuth ~47°) at ~25 ms^{-1}. Figure 1d shows a similar set of

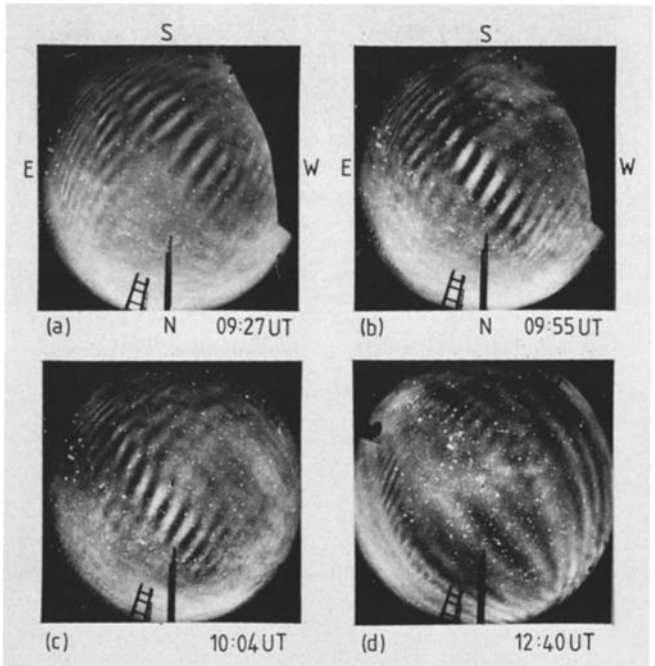

Figure 1. Four all-sky images showing the OI(557.7 nm) wave patterns (integration time 90s). Images a,b,c show the extent and apparent lateral motion of the small-scale wave pattern that was most conspicuous during the period 08:30-10:30 UT. Image d shows the morphology of the larger scale gravity wave at 12:40 UT.

small-scale waves (imaged ~3 hours later), superposed with an extensive, nearly orthogonal band pattern exhibiting a $\lambda_h = 38 \pm 2$ km and $v_h = 34 \pm 3$ ms^{-1} moving towards the SW (azimuth ~234°). Figure 3 shows the Na(589.2 nm) and O_2(0,1) data corresponding closely to the OI images at 09:55 UT and 12:40 UT. These emissions occur at ~90 and ~94 km altitudes respectively, and can be used to assess the vertical structure of the two wave motions.

MF Radar Wind Profiles

Figure 4 shows profiles of the horizontal winds obtained with the MF radar for 3-hour intervals centered at 09:30 UT and 12:30 UT

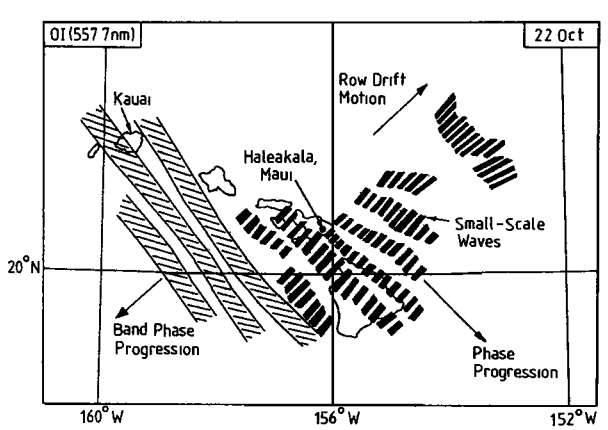

Figure 2. Map showing the horizontal scale size and geographical extent of the small-scale waves imaged at 09:27 UT (assuming an emission height of 96 km). The arrows indicate the observed phase progression towards the SE and the apparent drift motion of the rows towards the NE. For comparison three of the larger scale bands evident in Figure 1d are also plotted.

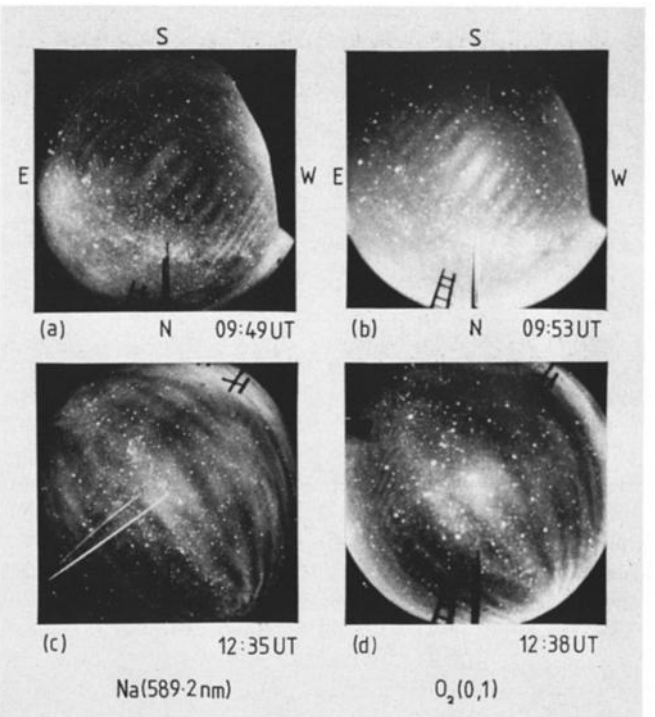

Figure 3. Four all-sky images showing wave structure in the Na and O_2 images at 09:50 UT and 12:40 UT.

and projected into the observed directions of motion of the two wave patterns of Figure 1 (i.e. toward the SE and SW). In Figure 4a winds of ~25 to 35 ms^{-1} towards the NW existed over all emission altitudes, opposite to the direction of the small-scale wave motion, suggesting an intrinsic phase speed of ~70 ms^{-1} and an intrinsic period of ~4.5 min. Winds toward the SW during this period were ≤10 ms^{-1}. The profiles of Figure 4b reveal a mean wind towards the N, with a component directed opposite to the observed phase motion of the large scale wave of ~20-30 ms^{-1}, implying an intrinsic phase speed of ~60 ms^{-1} and an intrinsic period of ~10.6 min.

Implications for Wave Dynamics

Short Wavelength Motions

Inspection of the image data of Figures 1 and 3 reveals a number of interesting properties. One important feature is the high degree of correlation between the small-scale waves imaged at different altitudes. Comparison of the early OI, Na and O_2 (and OH) waves show close alignment at the zenith when compensation was made for the slightly different times of the three images. This suggests a wave motion with little or no phase variation with altitude, such as expected for motions ducted near a local maximum of horizontal velocity or stability [Chimonas and Hines, 1986; Fritts and Yuan, 1989]. Detailed analysis (not shown) also suggests a phase retardation of the upper layers relative to those below, which appears symmetric about the zenith, indicating that this wave motion was vertically coherent across the sky.

Vertical phase coherence by itself provides persuasive evidence for ducted gravity waves, but there are other data that further support this case. These are the radar wind profiles shown in Figure 4, the first of which indicates a large negative mean wind in the direction of phase progression below ~98 km. With a λ_h of 19 km, a scale height H ~6 km and an assumed static stability $N^2 \sim 2 \times 10^{-4}$ s^{-2}, we infer from the Taylor-Goldstein equation a vertical wavenumber (m) squared given by

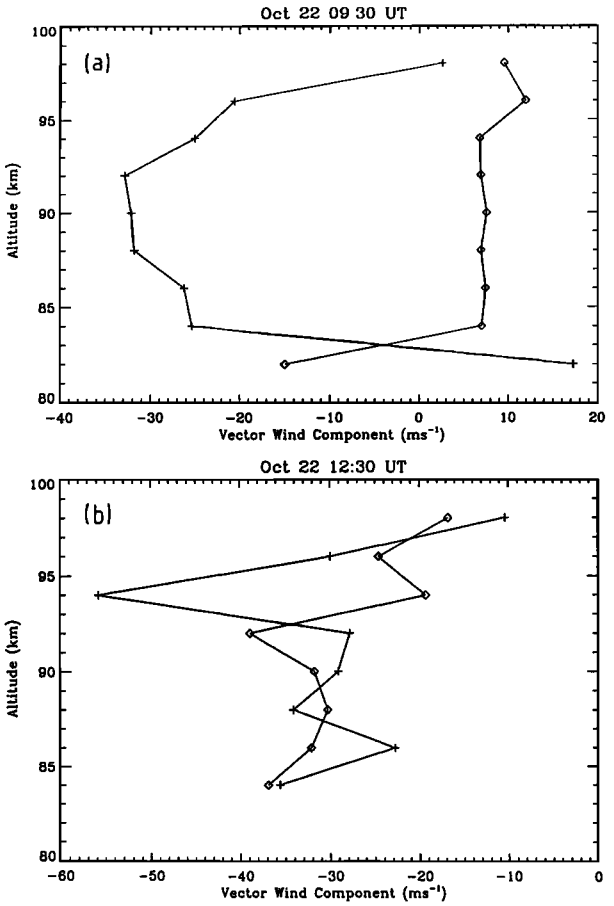

Figure 4. Time averaged wind measurements determined by the MF radar. The crosses show the SE-ward wind component in the direction of motion of the small-scale waves, and the diamonds the SW-ward wind component in the direction of motion of the bands.

$$m^2 = N^2/(c-u)^2 - k^2 - 1/4H^2 \quad (1)$$

where we have neglected shear and curvature effects of the mean wind profile and c is the observed phase speed, u is the mean wind in the direction of wave motion and k is the horizontal wave number. When $m^2 > 0$ the motion is vertically propagating, when $m^2 < 0$ the wave is vertically evanescent. Eq.(1) thus allows us to compute how large an intrinsic phase speed (c-u) is required for evanescent (or ducted) behavior. In this case, a value of (c-u) ~50 ms^{-1} or larger is required. However, (c-u) values below ~96 km (where the emission layers occur) are typically 70 ms^{-1}. Thus, the suggestion that these motions represent ducted waves is also supported by the environmental data. A final feature of the observed structures supporting this interpretation is the intensity variation of the different nightglow features with height. This is shown in Figure 5 for the prominent small-scale waves observed around 09:55 UT. The larger response of the OI relative to the O_2 and Na features at lower altitudes is strongly suggestive of a wave duct at greater altitudes.

The morphology of these small-scale wave motions was most unusual and to our knowledge has not been previously reported [Taylor et al., 1995]. In particular, Figure 1 shows the wave forms to be staggered, with alternating bright and dark forms in adjacent rows (Figure 2). One possible explanation for this unusual pattern is the superposition of two band-type motions having similar characteristics, but slightly different directions of propagation i.e., similar periods, horizontal wavelengths and amplitudes, but somewhat different azimuths. For example, two identical waves with horizontal wavelengths of ~19 km propagating at phase speeds of ~40 ms^{-1} and ~20° apart, toward azimuths of 125° and 145° N, would produce a row-like pattern having an apparent wavelength of 19.3 km and phase speed of 40.6 ms^{-1}. Such a superposition would also account for the staggering of bright and dark forms in adjacent rows because the superposed motions would generate an interference pattern with a fringe spacing of, in this case 19 km/2Sin10° = 55 km, which is consistent with the observed separation between the bright forms in alternating rows. Furthermore, a slightly larger phase speed for the component propagating at 145° N would easily account for the apparent drift motion of the wave group towards the NE.

Long Wavelength Motions

The bands propagating towards the SW were evident for most of the night but were very prominent at later times. In this case, an intrinsic phase speed of ~60 ms^{-1} combined with a larger horizontal wavelength (~38 km) implies a large vertical wavelength (λ_z) of ~40 km. This wave is quite distinct from the evanescent character of the ducted wave discussed above and indicates a role for this motion in the vertical transport of energy and momentum. Further evidence of the vertical progression of this wave motion was again provided by the optical data which suggest a small phase shift with altitude consistent with a large λ_z. The orthogonal orientation of the smaller-scale waves to these bands is suggestive of a direct relationship between these two wave motions but the mechanism is not obvious. However, the horizontal wavelengths and lifetimes of the small-scale waves are too large to result from a convective instability induced by the long wavelength motion breaking as it propagated into the lower thermosphere [Fritts et al., 1993].

Summary

We have presented a preliminary analysis of the wave motions observed in the OI, Na and O_2 nightglow emissions on 22 October, 1993. This night was selected because of the distinct wave structures present and the availability of correlative MF radar wind data. The coherence of the small-scale waves over ~80-100 km altitude and their high intrinsic phase speed suggest a ducted motion

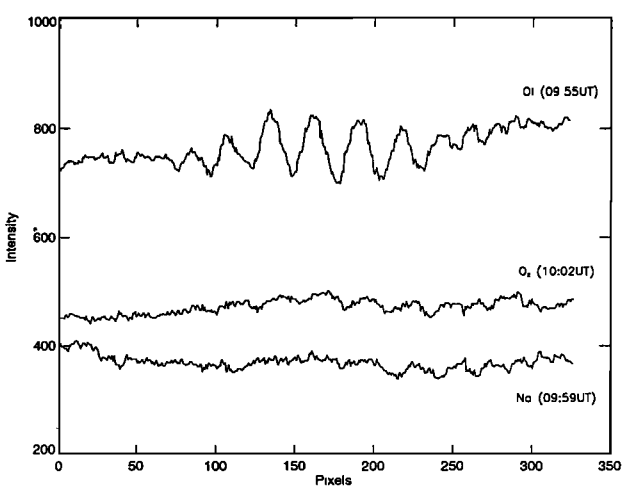

Figure 5. Intensity scan across the central, prominent, row around 09:55 UT for the OI, O_2 and Na emissions. The OI structures were most pronounced at ~7% modulation, with ~3% for the O_2 and only ~1% for the Na (the OH wave modulation was barely detectable).

with a vertically evanescent character at nightglow altitudes. The unusual morphology of these patterns discriminates them from small-scale "ripple" events and in this case an explanation for their appearance may lie in the interference of two comparable band-type motions progressing at closely spaced azimuths. Similar type small-scale waves were observed on several occasions during this campaign (primarily at OI wavelengths), and their orientations were also found to be near perpendicular to that of a concurrent larger scale wave pattern. A detailed study on the role of the larger scale wave motions will be made in due course. Together, these observations suggest an important capability for quantitative gravity wave studies combining optical measurements of wave structure over an extended altitude with simultaneous ground-based wind measurements.

Acknowledgments. This research was funded by the National Science Foundation (NSF) grant Nos ATM-9118899, ATM-9301981 and ATM-9302844. Operational support for the MF radar was also provided by the NSF under grant NSF93-02050. Partial support for the image analysis was provided by the Geophysics Directorate, Air Force Phillips Laboratory, contract No F19628-93-C-0165. The assistance of J.A. Albetski and V. Taylor are gratefully acknowledged.

References

Chimonas, G., and C.O. Hines, Doppler ducting of atmospheric gravity waves, *J. Geophys. Res., 91*, 1219-1230, 1986.

Clairemidi, J., M. Herse, and G. Moreels, Bi-dimensional observation of waves near the mesopause at auroral latitudes, *Planet. Space Sci., 33*, 1013-1022, 1985.

Fritts, D.C., J.R. Isler, G. Thomas, and Ø. Andreassen, Wave breaking signatures in noctilucent clouds, *Geophys. Res. Lett., 20*, 2039-2042, 1993.

Fritts, D.C., A review of gravity wave saturation processes, effects, and variability in the middle atmosphere, *Pageoph, 130*, 343-371, 1989.

Fritts and Yuan, An analysis of gravity wave ducting in the atmosphere: Eckart's resonances in thermal and Doppler ducts, *J. Geophys. Res., 94*, 18455-18466, 1989.

Hines, C.O., Internal atmospheric gravity waves at ionospheric heights, *Can. J. Phys., 38*, 1441-1481, 1960.

Isler, J.R., and D.C. Fritts, Mean winds and tidal and planetary wave motions over Hawaii during ALOHA-93, *Geophys. Res. Lett.*, this issue, 1995.

Peterson, A.W., Airglow events visible to the naked eye, *Appl. Optics, 22*, 3390-3393, 1979.

Taylor, M.J., M. B. Bishop, and V. Taylor, All-sky measurements of short period waves imaged in the OI(557.7 nm), Na(589.2 nm) and near infrared OH and O_2(0,1) nightglow emissions during the ALOHA-93 campaign, *Geophys. Res. Lett.*, this issue, 1995.

Taylor, M.J., and M.A. Hapgood, On the origin of ripple-type wave structure in the OH nightglow emission, *Planet. Space Sci., 38*, 1421-1430, 1990.

Taylor, M.J., M.A. Hapgood, and P. Rothwell, Observations of gravity wave propagation in the OI (557.7 nm), Na (589.2 nm) and the near infrared OH nightglow emission, *Planet. Space Sci., 35*, 413-427, 1987.

M.J. Taylor, Space Dynamics Laboratory, Utah State University, Logan, UT 84322-4145 (e-mail: Taylor@psi.sci.sdl.usu.edu).

D.C. Fritts and J.R. Isler, Laboratory for Atmospheric and Space Physics, Campus Box 392, University of Colorado, Boulder, CO 80309-0392 (e-mail: Dave@michelangelo.colorado.edu, and Joe@leonardo.colorado.edu).

(Received December 7, 1994; revised August 9, 1995; accepted August 25, 1995)